J. Phys. B: Atom. Molec. Phys., Vol. 7, No. 13, 1974. Printed in Great Britain.

The application of first order many-body theory to the calculation of the differential and integral cross sections for the electron impact excitation of the 2^1S, 2^1P, 2^3S, 2^3P states of helium

L D Thomas†, Gy Csanak, H S Taylor and B S Yarlagadda

Department of Chemistry, University of Southern California, Los Angeles, California 90007, USA

† IBM Research Laboratory, San Jose, California 95114, USA

Received 8 October 1973

Abstract. The first order form of the many-body theory for inelastic scattering (called random phase approximation) has been applied in the 29·6 eV $\leqslant$ E $\leqslant$ 81·63 eV energy region for the electron impact excitation of the 2^1S, 2^1P, 2^3S, 2^3P states of helium. Differential and integral cross sections are calculated and compared with recent experiments. The results for each state are discussed and compared with other calculations.

1. Introduction

In a recent series of papers (Csanak *et al* 1971, Csanak *et al* 1973, to be referred to in the future as I and II respectively), the many-body theory of Martin and Schwinger (1959) has been used to derive first and second order theories for the computation of electron–atom (molecule) inelastic scattering cross sections. The first order theory was called the random phase approximation (RPA).

In the present paper the first order (or RPA) results are given for application to inelastic electron scattering from the ground state of helium to the four excited states, 2^1S, 2^1P, 2^3S and 2^3P.

2. Theory

2.1. The RPA inelastic scattering matrix

The RPA inelastic scattering matrix is given in the following form (see II)

$$S^{\mathrm{RPA}}_{nq,0p} = -2\pi i\delta(\epsilon_p - \epsilon_q - \omega_n) \int \mathrm{d}x\, \mathrm{d}y f_q^{(-)*\mathrm{HF}}(x) V^{\mathrm{RPA}}_{0n}(x, y) f_p^{(+)\mathrm{HF}}(y) \qquad (1)$$

where p and q refer to the quantum numbers (momentum, spin) of the incoming and

outgoing electrons, with energies ϵ_p and ϵ_q respectively; x and y denotes both the spatial and spin coordinates of the electrons, 0 refers to the initial (ground state and n to the final (excited) state of the target. ($\omega_n = E_n - E_0$ is the excitation energy.)

$V_{0n}^{\text{RPA}}(x, y)$ is the transition potential in the RPA and is given as

$$V_{0n}^{\text{RPA}}(x, y) = \delta(x-y)\int \frac{1}{|\boldsymbol{x}-\boldsymbol{y}'|} X_n^{\text{RPA}}(y', y')\,\mathrm{d}y' - \frac{1}{|\boldsymbol{x}-\boldsymbol{y}|} X_n^{\text{RPA}}(y, x) \tag{2}$$

where $X_n^{\text{RPA}}(y, x)$ is the RPA value of the transition density matrix between the states n and 0. ($\boldsymbol{x}$ and $\boldsymbol{y}$ are the spatial parts of x and y respectively.)

$X_n^{\text{RPA}}(y, x)$ can be obtained by solving the RPA eigenvalue equation. (See Schneider *et al* 1970, Schneider 1970, Yarlagadda *et al* 1973, in this context.)

$f_p^{(+)\text{HF}}(y)$ and $f_q^{(-)\text{HF}}(x)$ are the Hartree–Fock (HF) continuum (virtual) orbitals with outgoing wave and incoming wave boundary conditions respectively.

2.2. *Comments on the RPA formula*

$S_{nq,0p}^{\text{RPA}}$ is a first order formula and connects only the initial and final channels. V_{0n}^{RPA} is exactly analogous to the static exchange (or HF) optical potential of elastic scattering, except that the RPA transition density (density matrix) replaces the HF ground-state density (density matrix). Most unusual about equation (1) is that the HF virtual orbital of proper final momentum appears for the outgoing electron (and therefore corresponds to an electron moving in the field of the ground state target). This is in contrast to distorted wave methods where the electron leaves in the field of the final state. Madison and Shelton (1973) in a program of computation devoted to studying the distorted wave method discovered that the replacement of the final state field by that of the initial state gave improved results for most energies. This scheme (called FG), which is essentially identical to the RPA formula, as given by equations (1) and (2), has fulfilled the orthogonality requirement between channels which has been imposed by them. The orthogonality requirement of Madison and Shelton (1973) was adopted for the practical reason of reducing a multi-particle form of the distorted-wave approximation to a computationally tractable form. The only orthogonality which can be theoretically required is the one referring to the total scattering states in the identical boundary conditions. It can be shown (Csanak 1974) that the RPA does indeed fulfill this requirement. One can probably infer that this condition is a property that should not be ignored by any approximation.

2.3. *Numerical calculation*

The analysis of equation (1) into a form that makes angular momentum and spin couplings explicit is given in a paper by Thomas *et al* (1974). The angular momentum and spin analysis of the RPA equation is already available in the literature (Altick and Glassgold 1964, Dunning and McKoy 1967, Shibuya and McKoy 1970).

The solution of the RPA eigenvalue equation has been done on a basis of 12s, 12p, 12d Slater-type orbitals and is described in the paper of Yarlagadda *et al* (1973). The HF functions that enter the RPA equation have been calculated from the basis set with the program kindly provided to us by Nesbet (1963, 1969).

The $f_p^{(+)\text{HF}}$ and $f_q^{(-)\text{HF}}$ orbitals are computed numerically by a program developed for more general purposes (Thomas 1973). The evaluation of the cross section is done

by the following equation:

$$\frac{d\sigma}{d\Omega} = \begin{cases} \dfrac{|q|}{4\pi^2|p|}\tfrac{1}{2}|2T_D - T_E|^2 & \text{singlet excitation} \quad (3a) \\ \dfrac{|q|}{4\pi^2|p|}\tfrac{3}{2}|T_E|^2 & \text{triplet excitation} \quad (3b) \end{cases}$$

here

$$T_D = \int dx\, dy f_q^{(-)HF^*}(x) f_p^{(+)HF}(x) \frac{1}{|x-y|} X_{nLMS}^{RPA}(y, y) \quad (4a)$$

and

$$T_E = \int dx\, dy f_q^{(-)HF^*}(x) f_p^{(+)HF}(y) \frac{1}{|x-y|} X_{nLMS}^{RPA}(y, x) \quad (4b)$$

where $f_q^{(-)HF}(x)$ and $f_p^{(+)HF}(y)$ are the spatial parts of the HF virtual orbitals (q and p refer to momentum quantum numbers and $|q|$ and $|p|$ mean the magnitude of these momenta) and $X_{nLMS}^{RPA}(y, x)$ is the properly normalized spatial part of the RPA transition density matrix ($nLMS$ refer to principal, angular momentum and total spin quantum numbers of the excited state respectively.) When the ground state is a singlet S, the spin factorization is given by (Yarlagadda 1973)

$$X_{nLMSM_s}^{RPA}(y\sigma, x\sigma') = X_{nLMS}^{RPA}(y, x)\xi_{SM_s}(\sigma, \sigma') \quad (4c)$$

with

$$\xi_{00}(\sigma, \sigma') = \frac{1}{\sqrt{2}}[\alpha^*(\sigma)\alpha(\sigma') + \beta^*(\sigma)\beta(\sigma')] \quad (4d)$$

$$\xi_{10}(\sigma, \sigma') = \frac{1}{\sqrt{2}}[\alpha^*(\sigma)\alpha(\sigma') - \beta^*(\sigma)\beta(\sigma')] \quad (4e)$$

$$\xi_{1-1}(\sigma, \sigma') = \beta^*(\sigma)\alpha(\sigma') \quad (4f)$$

$$\xi_{11}(\sigma, \sigma') = \alpha^*(\sigma)\beta(\sigma') \quad (4g)$$

where α and β are the usual spin functions.

It suffices to say here that the cross section calculation (ie the calculation of integrals in equations (4*a*) and (4*b*)) was done numerically and the times and difficulties are comparable to a first order Born calculations in partial wave form.

In summary, the computation reduces to (i) the solution of the HF and RPA eigenvalue equations on a basis set, (ii) numerical calculation of the HF continuum orbitals and (iii) numerical evaluation of the integrals involved in equations (4*a*) and (4*b*). The details are given by Thomas *et al* (1974).

3. Results

The results are given in the tables and figures. An attempt was made when possible and informative to give a representation, fair but certainly incomplete survey of previous

work.† The tables give a much more complete set of results than do the figures. The figures were selected from the tables for ease of discussion. Some further details are given in the paper of Thomas *et al* (1974).

3.1. The $1^1S \rightarrow 2^1P$ excitation

Table 1 and figures 1, 2, 3 and 4 give the computed results. In table 1 and figure 3 the cross sections for the $M = 0$ (σ_{2P_0}) and the $M = \pm 1$ ($\sigma_{2P_{\pm 1}}$) magnetic sublevels are also given (the $M = 1$ curve is $\sigma_{2P_1} + \sigma_{2P_{-1}}$) along with the total differential cross section (sum over the sublevels).

In figures 1 and 2 the experimental results of Truhlar *et al* (1973) and Hall *et al* (1973) are compared with the Born and close-coupled (two state) calculations of Truhlar *et al* (1973), the calculation of Madison and Shelton (1973) (FG scheme) and the present results.

In figure 3 the experimental results of Opal and Beaty (1972) and Truhlar *et al* (1970) are compared with the projected Coulomb–Born (CW) and Born calculation of Hidalgo and Geltman (1972), the calculation of Madison and Shelton (1973) (scheme FG) and with the present results.

Total cross section data are given in table 1 and figure 4. The experimental results are from Donaldson *et al* (1972) and from de Jongh and van Eck (1971).

Table 1. Differential cross sections for excitation of the 2^1P_M states of He. Columns labelled $M = 1$ are twice the 2^1P_1 cross section†

θ (degrees)	E(eV) units	29·6 $10^{-4}a_0^2$		40·1 $10^{-4}a_0^2$		55·5 $10^{-4}a_0^2$		81·63 $10^{-4}a_0^2$	
		$M = 0$	$M = 1$	$M = 0$	$M = 1$	$M = 0$	$M = 1$	$M = 0$	$M = 1$
0		13^{+2}	0	58^{+2}	0	15^{+3}	0	32^{+3}	0
10		11^{+2}	74	36^{+2}	72^{+1}	58^{+2}	28^{+2}	53^{+2}	62^{+2}
20		58^{+1}	17^{+1}	11^{+2}	90^{+1}	93^{+1}	17^{+2}	41^{+2}	16^{+2}
30		23^{+1}	17^{+1}	24^{+1}	50^{+1}	13^{+1}	52^{+1}	50	28^{+1}
40		68	12^{+1}	37	21^{+1}	27	13^{+1}	24	43
50		12	69	88^{-1}	76	23	34	22	67^{-1}
60		13^{-2}	37	14	30	25	10	19	18^{-1}
70		22^{-1}	20	19	14	24	50^{-1}	15	15^{-1}
80		61^{-1}	12	21	86^{-1}	21	38^{-1}	12	16^{-1}
90		88^{-1}	79^{-1}	21	63^{-1}	18	35^{-1}	42^{-1}	17^{-1}
100		10	56^{-1}	20	55^{-1}	15	33^{-1}	76^{-1}	17^{-1}
110		10	43^{-1}	19	45^{-1}	14	31^{-1}	66^{-1}	16^{-1}
120		11	33^{-1}	18	40^{-1}	13	27^{-1}	62^{-1}	14^{-1}
130		11	25^{-1}	18	31^{-1}	13	22^{-1}	61^{-1}	11^{-1}
140		11	17^{-1}	18	24^{-1}	14	16^{-1}	63^{-1}	77^{-2}
150		11	10^{-1}	19	14^{-1}	14	10^{-1}	65^{-1}	48^{-2}
160		11	48^{-2}	20	71^{-2}	15	48^{-2}	67^{-1}	22^{-2}
170		11	12^{-2}	20	14^{-2}	15	13^{-2}	68^{-1}	54^{-3}
180		11	0	20	0	15	0	68^{-1}	0
Total		706	409	156^{+1}	103^{-1}	202^{+1}	158^{+1}	197^{+1}	197^{+1}

† A superscript indicates the power of ten by which the entry should be multiplied.

† For complete reviews, see Moiseiwitch and Smith (1968), Trajmar (1973), Truhlar *et al* (1973), Madison and Shelton (1973), Rice *et al* (1972), Truhlar *et al* (1970), Hall *et al* (1973), Truhlar *et al* (1971).

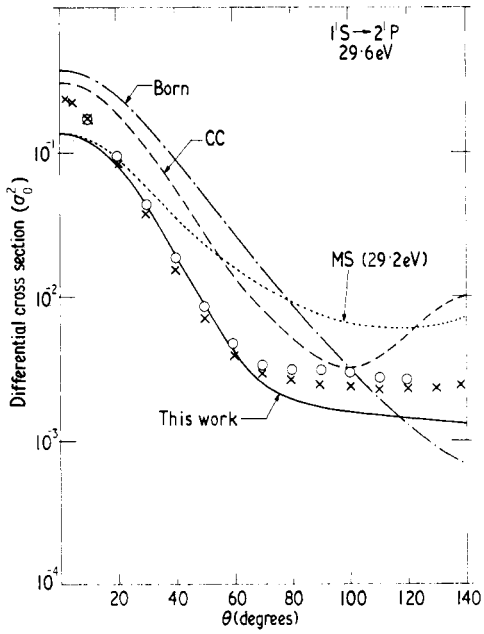

Figure 1. Theoretical and experimental cross sections for electron impact excitation of the 2^1P state of helium at an incident energy of 29·6 eV. Born Born calculation (Truhlar *et al*). CC Close coupling calculation (Truhlar *et al*). MS The calculation of Madison and Shelton. × Experiment (Truhlar *et al*). ○ Experiment (Hall *et al*).

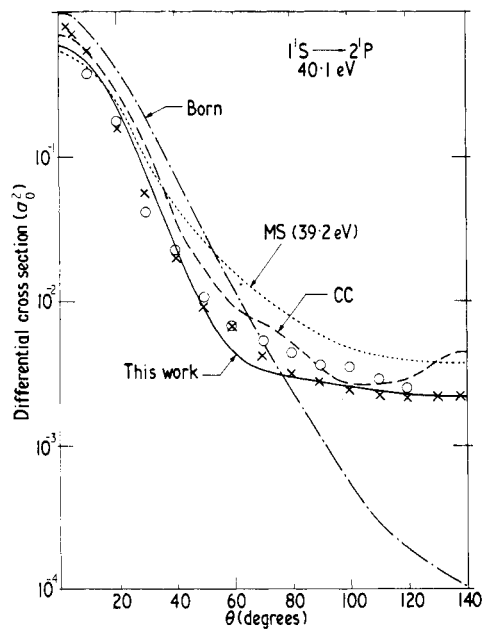

Figure 2. Same as figure 1 except here the energy is 40·1 eV.

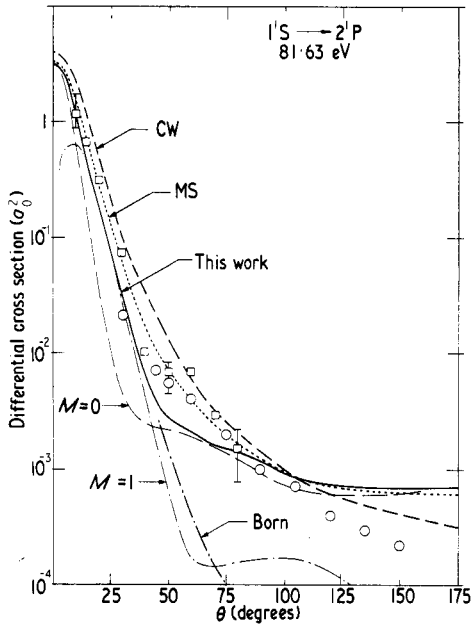

Figure 3. Same as figure 1 except here the energy is 81·63 eV. $M = 0$: the excitation cross section for the $M = 0$ sublevel. $M = 1$: twice the excitation cross section for the $M = 1$ sublevel. CW Coulomb projected Born approximation (Hidalgo and Geltman). MS The calculation of Madison and Shelton. Born Born approximation (Hidalgo and Geltman). ○ Experiment (Opal and Beaty). □ Experiment (Truhlar *et al*).

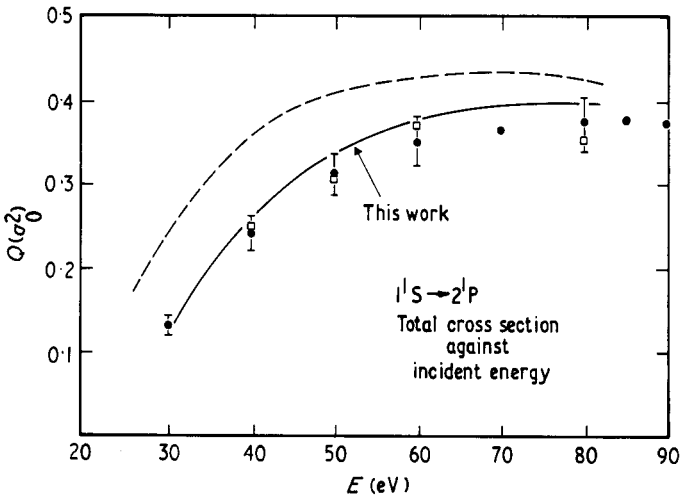

Figure 4. Comparison of theoretical and experimental integral cross section results for the excitation of the 2^1P state of helium. – – – The calculation of Madison and Shelton. □ Experiment (Donaldson *et al*). ● Experiment (de Jongh and van Eck).

3.2. The $1^1S \rightarrow 2^1S$ excitation

Table 2 and figures 5–7 give the results of the present (RPA) calculations along with the experimental results of Trajmar (1973) and Hall *et al* (1973) and with results of the Born (Rice *et al* 1972), (Shelton *et al* 1973) and Glauber (Yates and Tenney 1972) calculations.

Figure 8 is a second order result with an adiabatic, semiempirical, transition polarization potential (Truhlar *et al* 1971, Rice *et al* 1972, Csanak and Taylor 1973b). The form of the adiabatic transition polarization potential was chosen as the one given by Csanak and Taylor (1973b). The value of the transition polarizability was taken from Drake (1972) as $\alpha = 1{\cdot}584a_0^3$. The adiabatic approximation is expected to be good only for small angles, therefore the result only in that angular region is given.

Figure 9 compares the experimental and theoretical results for the total cross section. The experimental results are those of Vriens *et al* (1968) and Rice *et al* (1972). The theoretical results are those of the Born calculation of Rice *et al* (1972) and the projected Coulomb–Born calculation of Hidalgo and Geltman (1972).

3.3. The $1^1S \rightarrow 2^3S$ and $1^1S \rightarrow 2^3P$ excitations

Table 3 and 4 and figures 10–12 and 13–15 give the results for the excitation of the 2^3S and 2^3P states respectively. The experimental results are those of Crooks *et al* (1972), Jobe and St John (1967), Trajmar (1973) and Hall *et al* (1973) along with the Born–Oppenheimer (BO) calculation of Steelhammer (1971) and the calculation of Shelton *et al* (1973).

Table 2. Differential cross sections for the excitation of the 2^1S state of He†

θ (degrees)	E(eV) units	21.79 $10^{-4}a_0^2$	26·5 $10^{-4}a_0^2$	29·6 $10^{-4}a_0^2$	34·0 $10^{-4}a_0^2$	40·1 $10^{-4}a_0^2$	44·0 $10^{-4}a_0^2$	55·5 $10^{-4}a_0^2$	81·63 $10^{-4}a_0^2$	400 $10^{-4}a_0^2$	500
0		68	12^{+1}	21^{+1}	35^{+1}	49^{+1}	58^{+1}	79^{+1}	11^{+2}	17^{+2}	16^{+2}
10		68	11^{+1}	19^{+1}	31^{+1}	43^{+1}	50^{+1}	66^{+1}	85^{+1}	60^{+1}	47^{+1}
20		58	87	14^{+1}	22^{+1}	28^{+1}	32^{+1}	38^{+1}	39^{+1}	40	22
30		48	56	85	12^{+1}	14^{+1}	15^{+1}	15^{+1}	12^{+1}	43^{+1}	49^{-1}
40		37	28	37	44	50	51	50	40	71^{-2}	24^{-1}
50		27	90	95^{-1}	98^{-1}	14	17	23	25		
55		23	37^{-1}	29^{-1}	40^{-1}	94^{-1}	13	21	24		
60		21	95^{-2}	29^{-2}	32^{-1}	99^{-1}	14	23	25		
65		19	37^{-2}	88^{-2}	56^{-1}	13	18	26	25		
70		18	16^{-1}	38^{-1}	10	19	24	30	25		
80		20	79^{-1}	14	22	31	34	35	24		
90		26	17	27	34	41	42	37	22		
100		35	27	39	47	50	48	38	20		
110		46	37	50	58	57	52	38	18		
120		57	47	60	68	62	56	38	17		
130		68	53	68	75	66	58	38	16		
140		79	59	74	80	69	60	38	15		
150		87	64	79	82	70	62	40	15		
160		53	67	82	82	72	63	41	14		
170		97	69	84	82	72	64	41	14		
Total		552^{-1}	415	578	711	782	796	771	640		

† A superscript indicates the power of ten by which the entry should be multiplied.

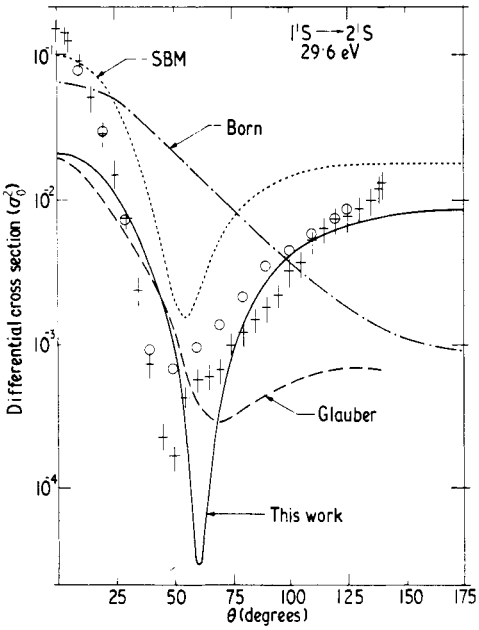

Figure 5. Theoretical and experimental cross sections for electron impact excitation of the 2^1S state of helium at an incident energy of 29·6 eV. SBM The calculation of Shelton, Baluja and Madison. Born approximation (Rice *et al*). Glauber approximation (Yates and Tenney). + Experiment (Trajmar). ○ Experiment (Hall *et al*).

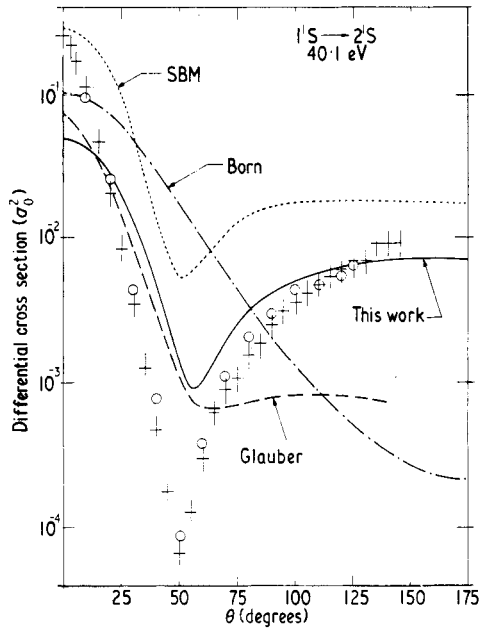

Figure 6. Same as figure 5 except here the energy is 40·1 eV.

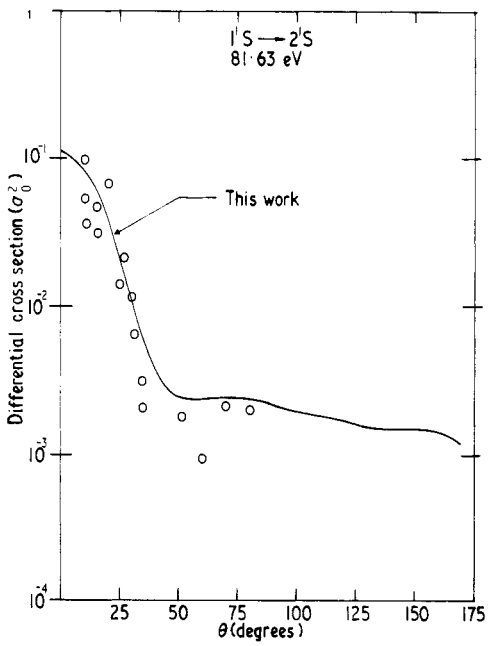

Figure 7. Same as figure 5 except here the energy is 81·63 eV. ○ Experimental results of Rice *et al.*

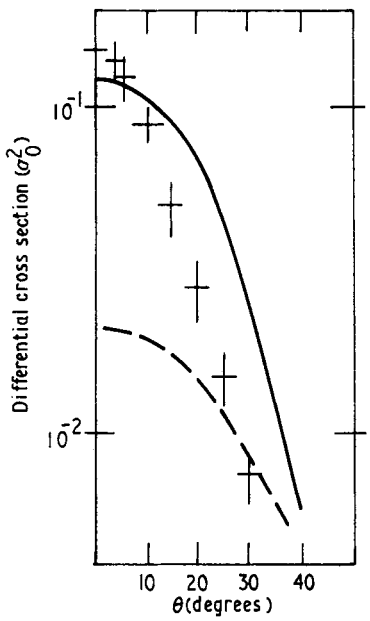

Figure 8. Same as figure 5 except the present calculation (solid curve) includes adiabatic transition polarization potential (Csanak and Taylor).

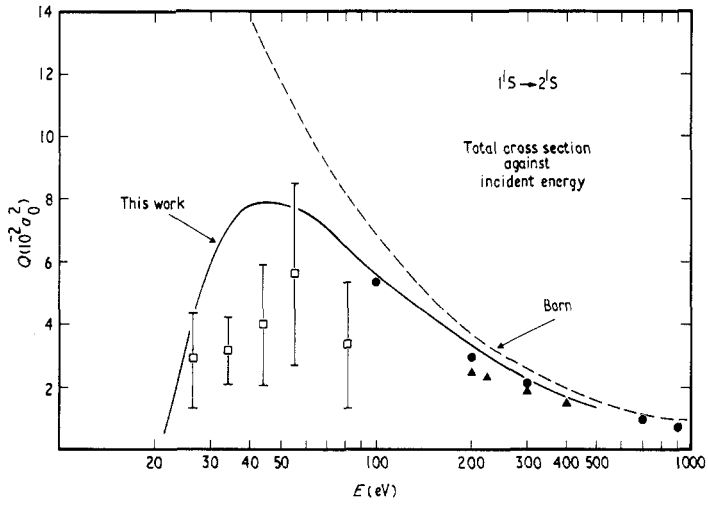

Figure 9. Comparison of theoretical and experimental integral cross section results for the excitation of the 2^1S state of helium. Born Born approximation (Rice *et al*). ● Coulomb projected Born approximations (Hidalgo and Geltman). □ Experiment (Rice *et al*). ▲ Experiment (Vriens *et al*).

Table 3. Differential cross sections for excitation of the 2^3S state of He†

θ (degrees)	E(eV) units	29·6 $10^{-4}a_0^2$	40·1 $10^{-4}a_0^2$	45 $10^{-4}a_0^2$	50 $10^{-4}a_0^2$	55 $10^{-4}a_0^2$	60 $10^{-4}a_0^2$	65 $10^{-4}a_0^2$	70 $10^{-4}a_0^2$	100 $10^{-4}a_0^2$	400 $10^{-6}a_0^2$	500 $10^{-6}a_0^2$
0		36^{+1}	21^{+1}	17^{+1}	14^{+1}	11^{+1}	94	79	67	27	19	32
10		34^{+1}	19^{+1}	15^{+1}	12^{+1}	94	77	64	53	21	94	86
20		28^{+1}	14^{+1}	98	73	56	45	37	31	15	23^{+1}	14^{+1}
30		22^{+1}	80	52	37	28	24	21	20	17	12^{+1}	61
40		16^{+1}	43	26	19	17	17	18	19	17	44	24
50		11^{+1}	24	15	13	14	15	16	17	13	12	92^{-1}
60		84	16	11	11	12	13	13	13	92^{-1}	38^{-1}	47^{-1}
70		67	15	11	11	11	11	11	11	66^{-1}	21^{-1}	29^{-1}
80		58	19	15	13	12	12	11	10	54^{-1}		
90		56	27	22	19	17	15	13	12	56^{-1}		
100		58	39	34	29	25	21	18	16	64^{-1}		
110		63	54	48	41	34	29	24	20	73^{-1}		
120		71	71	63	54	45	38	31	25	85^{-1}		
130		80	89	80	68	57	46	38	31	99^{-1}		
140		90	11^{+1}	96	81	67	55	44	36	11		
150		98	12^{+1}	11^{+1}	92	76	61	49	40	11		
160		10^{+1}	13^{+1}	12^{+1}	10^{+5}	82	66	53	43	12		
170		11^{+1}	14^{+1}	13^{+1}	11^{+1}	87	70	56	45	13		
180		11^{+1}	14^{+1}	13^{+1}	11^{+1}	87	72	57	46	13		
Total		1220	728	600	502	425	363	311	269	122	282	146

† A superscript indicates the power of ten by which the entry should be multiplied.

Table 4. Differential cross sections for excitation of the 2^3P_M states of He. Columns labelled $M = 1$ are twice the 2^3P_1 cross section†

θ (degrees)	E(eV) units	29·6 $10^{-3}a_0^2$		40·1 $10^{-3}a_0^2$		55·5 $10^{-4}a_0^2$		81·63 $10^{-5}a_0^2$	
		$M = 0$	$M = 1$	$M = 0$	$M = 1$	$M = 0$	$M = 1$	$M = 0$	$M = 1$
0		47	0	57	0	35^{+1}	0	15^{+2}	0
10		45	13^{-1}	54	21^{-1}	33^{+1}	21	13^{+2}	18^{+1}
20		40	45^{-1}	46	65^{-1}	26^{+1}	59	99^{+1}	40^{+1}
30		31	82^{-1}	35	10	19^{+1}	74	63^{+1}	37^{+1}
40		23	11	25	11	12^{+1}	67	36^{+1}	24^{+1}
50		16	13	16	10	74	50	20^{+1}	13^{+1}
60		11	13	10	91^{-1}	44	34	11^{+1}	69
70		84^{-1}	12	65^{-1}	74^{-1}	27	23	65	37
80		87^{-1}	11	52^{-1}	58^{-1}	20	16	47	21
90		11	93^{-1}	55^{-1}	46^{-1}	19	11	42	14
100		16	78^{-1}	68^{-1}	36^{-1}	21	84^{-1}	43	99^{-1}
110		21	63^{-1}	88^{-1}	28^{-1}	25	64^{-1}	47	78^{-1}
120		27	49^{-1}	11	21^{-1}	30	49^{-1}	53	62^{-1}
130		33	35^{-1}	13	15^{-1}	35	36^{-1}	59	47^{-1}
140		38	24^{-1}	15	10^{-1}	40	24^{-1}	65	33^{-1}
150		42	14^{-1}	17	60^{-2}	44	14^{-1}	70	20^{-1}
160		46	63^{-2}	19	28^{-2}	47	66^{-2}	73	94^{-2}
170		48	16^{-2}	19	71^{-3}	49	17^{-2}	76	24^{-2}
180		49	0	20	0	50	0	77	0
Total		281	97	176	64	719	266	200^{+1}	845

† A superscript indicates the power of ten by which the entry should be multiplied.

4. Discussion

4.1. The $1^1S \rightarrow 2^1P$ excitation

The calculations for this excitation are expected to be the best among the results presented in this paper. The reason for this lies in the strong coupling of the 2^1P (optically allowed) state to the 1^1S state. The differential and total cross sections are generally in very good agreement with experiment except at low energies (below 30 eV) and small angles (less than 15°). The results of Madison and Shelton (1973) differ from the present results primarily because of their approximate treatment of exchange in the HF continuum functions. Very accurate wavefunctions would be needed to get transition densities of RPA quality. Of great significance is the quality of this simple formula at such a low energy as 29·6 eV. (Within experimental accuracy in the $25° \leqslant \theta \leqslant 60°$ region.) Previous publications on first order methods have not given good results for first order theories below 80 eV. Of equal significance is the fact that the results are so good in the energy region where many open channels exist. It is important to observe that the labour and input, in terms of basis set etc, for the close-coupling calculations are significantly greater than those of this work and still the results are poorer (except for the possibility of obtaining resonances by close coupling).

At the energies studied here (for the 2^1P excitation the results improve with increasing energy) the principle error in the 2^1P cross sections are at small angles (less than 15°).

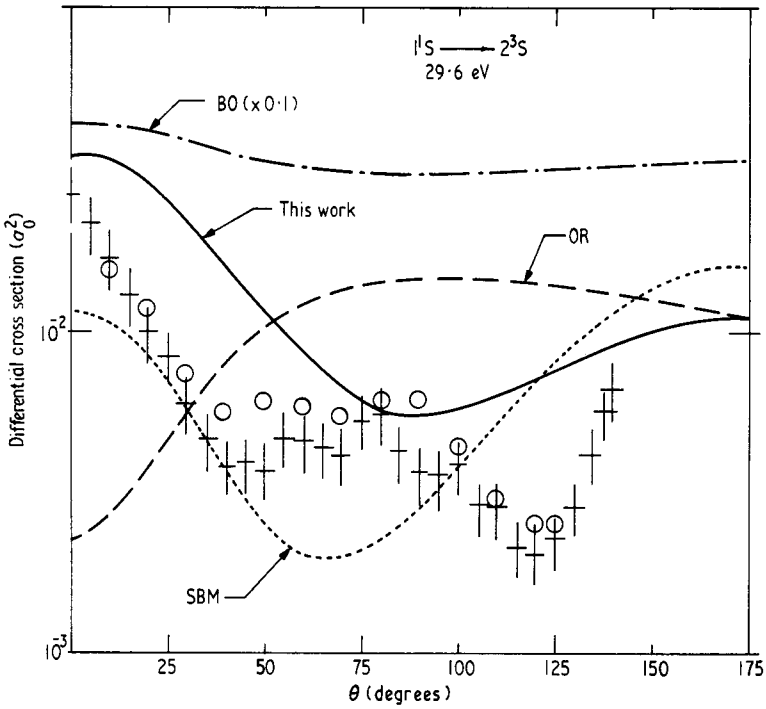

Figure 10. Theoretical and experimental cross sections for electron impact excitation of the 2^3S state of helium at an incident energy of 29·6 eV. BO Born–Oppenheimer approximation (Steelhammer). OR Ochkur–Rudge approximation (Steelhammer). SBM The calculation of Shelton, Baluja and Madison. + Experiment (Trajmar). ○ Experiment (Hall *et al*).

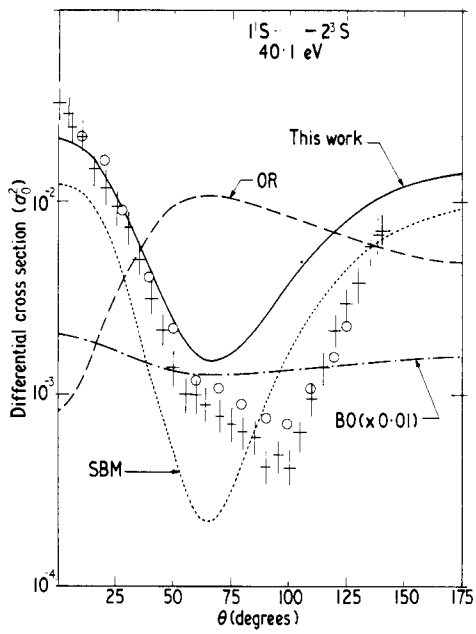

Figure 11. Same as figure 12 except here the energy is 40·1 eV.

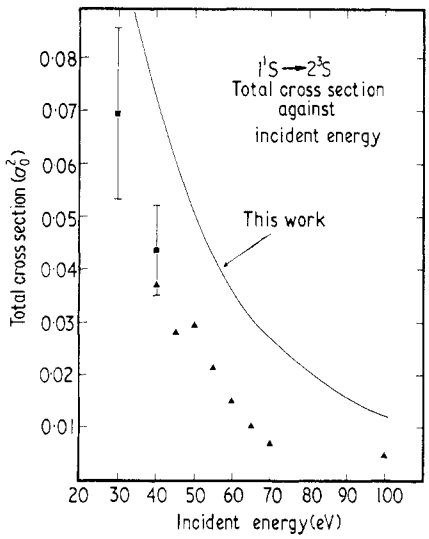

Figure 12. Comparison of theoretical and experimental integral cross section results for the excitation of 2^3S state of helium. — This work. ■ Experiment (Trajmar). ▲ Experiment (Crooks *et al*).

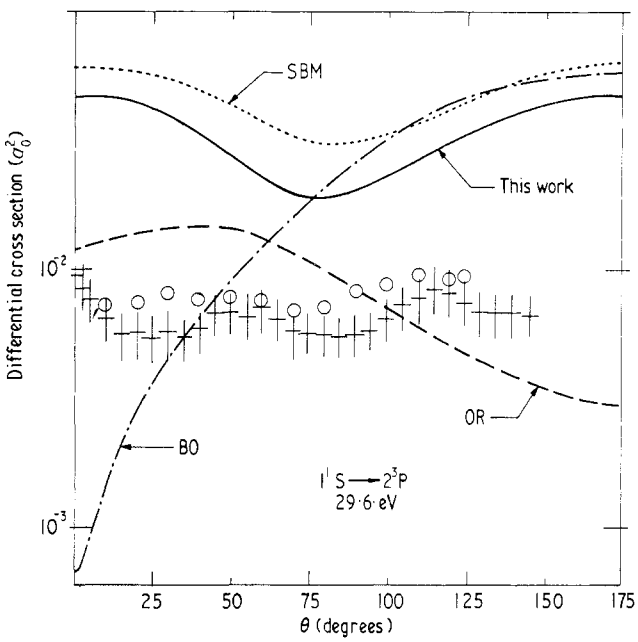

Figure 13. Theoretical and experimental cross sections for electron-impact excitation of the 2^3P state of helium at an incident energy of 29·6 eV. BO Born–Oppenheimer approximation (Steelhammer). OR Ochkur–Rudge approximation (Steelhammer). SBM The calculation Shelton, Baluja and Madison. + Experiment (Trajmar). ○ Experiment (Hall *et al*).

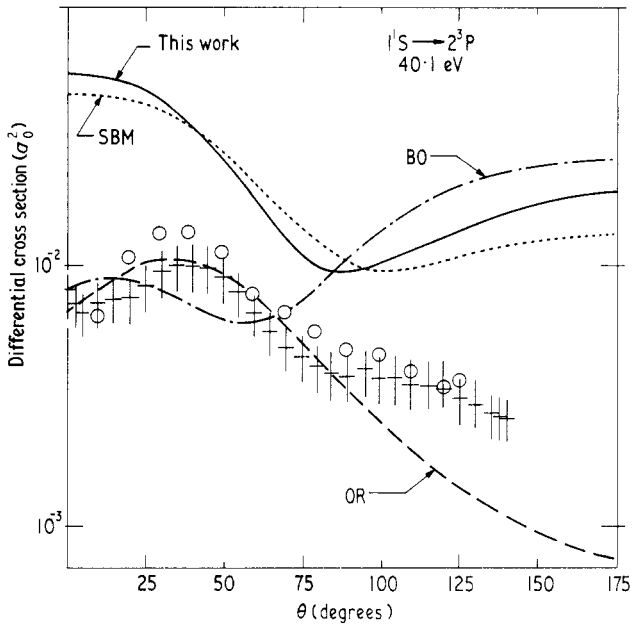

Figure 14. Same as figure 13 except here the energy is 40·1 eV.

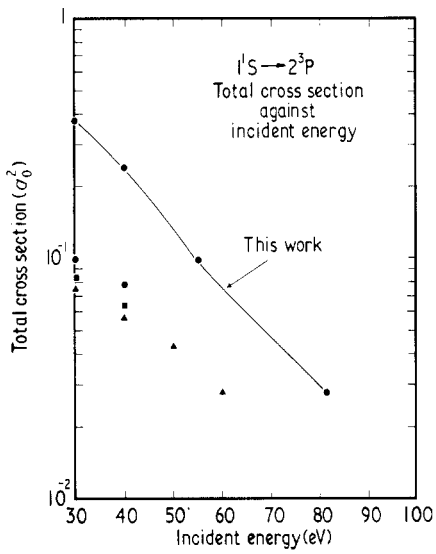

Figure 15. Comparison of theoretical and experimental integral cross sections results for the excitation of 2^3P state of helium. —This work. ● Experiment (Hall *et al*). ■ Experiment (Trajmar) ▲ Experiment (Jobe and St John).

This error is principally due to neglect of polarization in the transition potential as shall be discussed and demonstrated for the excitation of the 2^1S state.

Not shown here is the fact that the direct $|T_D|$ in equation (3*a*) makes by far the major contribution to the cross section. Exchange is not a major effect in this excitation process.

4.2. The $1^1S \rightarrow 2^1S$ excitation

The differential cross sections are quite good for this excitation as the figures show. The present theory clearly contains the essential physics of this transition.

One notes, as in the case of 2^1P excitation, the small angle error. This is of course due to long-range effects which are related to polarizabilities (Truhlar *et al* (1971), Rice *et al* (1972). Figure 8 shows that even an approximate, adiabatic evaluation of the second order polarization term increases the low-angle cross section. This is probably the main effect at low angle for all cross sections here presented. Of greater interest is that the total cross section is high. This indicates that coupling to other, open channels is needed to draw away flux.

The fact that the results of this work reproduce the 'dip' in the differential cross section (in about 5° accuracy) at about 50° is significant. The present calculation also gives the proper trend in the depth of the dip. (The dip is getting less shallow with increasing energy.) It is important to report also that the minimum exists strongly in the direct term T_D alone.

4.3. The excitation of the 2^3S and 2^3P states

The 2^3S and 2^3P excitations (both spin forbidden) will be discussed together. The results here are of considerably greater accuracy than previously computed results. The general shapes are correct, however, for the 2^3S and a factor of three for the 2^3P cross section at all energies the magnitude of the differential and total cross sections are too high by a factor of two.

Since the 2^3S and 2^3P states couple with each other as strongly as with the 1^1S state it is not surprising that a first order theory is not as successful as with the 2^1P case. A second order theory (Csanak *et al* 1973a) should yield greatly improved results.

5. Conclusion

The first order form of the many-body theory (the RPA) has been applied to the electron impact excitation of the $2^1S, 2^1P, 2^3S, 2^3P$, states of helium in the 29·6 eV $\leqslant E \leqslant$ 81·63 eV energy region. The best results have been obtained for the optically allowed excitation of the 2^1P states where experimentally accurate results were obtained over 40 eV in the whole angular range except for small angles (less than 15°). The results for the excitation of the 2^1S state are quite good. The main feature of the differential cross section (the strong dip around 50°) has been recovered. The cross sections seem to be experimentally accurate over 50 eV except the small angle region. For the excitation of the 2^3S and 2^3P states the gross features have been obtained. The magnitude of these cross sections are generally too high (about a factor of 2).

The RPA formula seems to be the most accurate first order 'distorted wave' type of expression. This has been justified by the cross sections reported here and a comparative study made by Madison and Shelton (1973).

Acknowledgments

The authors acknowledge the financial support of the National Science Foundation and the Presidents Fund of the California Institute of Technology.

They are very much indebted to Professor W N Shelton and Dr Baluja (The Florida State University, Tallahasse) for communicating their results on the 2^1S, 2^3S, 2^3P excitations prior to publication. They also thank Dr S Trajmar (Jet Propulsion Laboratory, Pasadena) and Dr R Hall (Laboratoire de Physique et Optique Corpusculaires, Universite de Paris, France) for providing the results of their measurement prior to publication. They are also grateful to Professor D G Truhlar (University of Minnesota) for communicating some of his unpublished calculations and to Dr R K Nesbet (IBM Corp., San Jose) for providing his Hartree–Fock program.

The authors acknowledge enlightening discussions with Professor R T Poe (University of California at Riverside) and Dr D C Cartwright (Aerospace Corporation).

References

Altick P L and Glassgold A E 1964 *Phys. Rev.* **133** 632–46
Crooks G B, DuBois R D, Golden D E and Rudd M E 1972 *Phys. Rev. Lett.* **29**, 327–9
Csanak Gy, Taylor H S and Yaris R 1971 *Phys. Rev.* A **3** 1322–8
Csanak Gy, Taylor H S and Tripathy 1973 *J. Phys.* B: *Atom molec. Phys.* **6** 2040–54
Csanak Gy and Taylor H S 1973 *J. Phys.* B: *Atom molec. Phys.* **6** 2055–71
Csanak Gy 1974 *J. Phys.* B: *Atom. molec. Phys.* **7** 1289–95
Donaldson F G, Hender M A and McConkey 1972 *J. Phys.* B: *Atom molec. Phys.* **5** 1192–210
Drake G W F 1972 private communication to Rice *et al* 1972
Dunning T H and McKoy V 1967 *J. chem. Phys.* 1735–47
Hall R I, Joyez G, Mazeau J, Reinhardt J and Scherman C 1973 *J. de Phys.* **34** 827–43
Hidalgo M D and Geltman S 1972 *J. Phys.* B *Atom molec. Phys.* **5** 617–26
Jobe J D and St John R M 1967 *Phys. Rev.* **164** 117
deJongh J P and Van Eck J 1971 *Abstr. 7th Int. Conf. on the Physics of Electronic and Atomic Collisions* (Amsterdam: North Holland) 701–3
Madison D H and Shelton W N 1973 *Phys. Rev.* A**7** 499–513
Martin P C and Schwinger J 1959 *Phys. Rev.* **115** 1342–73
Moiseiwitsch B L and Smith S J 1968 *Electron Impact Excitation of Atoms* NSRDS-NBS 25 (Washington: Natl. Bur. of Stand.)
Nesbet R K 1963 *Rev. Mod. Phys.* **35** 552–7
—— 1969 *IBM Research Report* RJ 572 (unpublished)
Opal C B and Beaty E C 1972 *J. Phys.* B: *Atom molec. Phys.* **5** 627–35
Rice J K, Truhlar D G, Cartwright D C and Trajmar S 1972 *Phys. Rev.* A**5** 762–82.
Schneider B, Taylor H S and Yaris R 1970 *Phys. Rev.* A **1** 855–67
Schneider B 1970 *Phys. Rev.* A **2** 1873–7
Shelton W N, Baluja K L and Madison D H 1973 *Abstr. 8th Int. Conf. on the Physics of Electronic and Atomic Collisions* (Beograd: Institute of Physics Beograd) 296–7
Shibuya T and McKoy V 1970 *Phys. Rev.* A **2** 2208–18
Steelhammer, J C 1971 *PhD Thesis* University of Minnesota
Thomas L D 1973 *J. comp. Phys.*
Thomas L D, Yarlagadda B S, Csanak Gy and Taylor H S 1974 *Comp. Phys. Commun.* **6** 316–30
Trajmar S 1973 *Phys. Rev.* A **8** 191–203
Truhlar D G, Rice J K, Kupperman A and Trajamr S and Cartwright D C 1970 *Phys. Rev.* A **1** 778–802
Truhlar D G, Rice J K, Trajmar S and Cartwright D C 1971 *Chem. Phys. Lett.* **9** 299–305
Truhlar D G, Trajmar S, Williams W, Ormonde S and Torres B 1973 *Phys. Rev.* A **8** 2475–82
Vriens L, Simpson J A and Mielczarek S R 1968 *Phys. Rev.* **165** 7–15
Yarlagadda B S 1973 *PhD Thesis*, University of Southern California (unpublished)
Yarlagadda B S, Csanak Gy, Taylor H S, Schneider B and Yaris R 1973 *Phys. Rev.* A **7** 146–54
Yates A C and Tenney A 1972 *Phys. Rev.* A **6** 1451–6